EBioMedicine 47 (2019) 184–194

Contents lists available at ScienceDirect

EBioMedicine

journal homepage: www.ebiomedicine.com

EBioMedicine
Published by THE LANCET

Research paper

Spleen tyrosine kinase activity regulates epidermal growth factor receptor signaling pathway in ovarian cancer

Yu Yu [a,b,*,1], Yohan Suryo Rahmanto [a,b], Yao-An Shen [a,b], Laura Ardighieri [b], Ben Davidson [c], Stephanie Gaillard [a], Ayse Ayhan [b,d], Xu Shi [e], Jianhua Xuan [e], Tian-Li Wang [a,b,f,*], Ie-Ming Shih [a,f,*]

[a] Sidney Kimmel Comprehensive Cancer Center, Johns Hopkins Medical Institutions, Baltimore, MD 21231, United States of America
[b] Department of Pathology, Johns Hopkins Medical Institutions, Baltimore, MD 21205, United States of America
[c] Department of Pathology, Oslo University Hospital and Institute of Clinical Medicine, Faculty of Medicine, University of Oslo, Norwegian Radium Hospital, 0310 Oslo, Norway
[d] Department of Pathology, Seirei Mikatahara Hospital, Hamamatsu and Hiroshima Universities Schools of Medicine, Hamamatsu 431-3192, Japan
[e] Bradley Department of Electrical and Computer Engineering, Virginia Polytechnic Institute and State University, Arlington, VA 22203, United States of America
[f] Department of Gynecology and Obstetrics, Johns Hopkins Medical Institutions, Baltimore, MD 21287, United States of America

ARTICLE INFO

Article history:
Received 13 June 2019
Received in revised form 14 August 2019
Accepted 23 August 2019
Available online 3 September 2019

ABSTRACT

Background: Spleen tyrosine kinase (SYK) is frequently upregulated in recurrent ovarian carcinomas, for which effective therapy is urgently needed. SYK phosphorylates several substrates, but their translational implications remain unclear. Here, we show that SYK interacts with EGFR and ERBB2, and directly enhances their phosphorylation.

Methods: We used immunohistochemistry and immunoblotting to assess SYK and EGFR phosphorylation in ovarian serous carcinomas. Association with survival was determined by Kaplan-Meier analysis and the log-rank test. To study its role in EGFR signaling, SYK activity was modulated using a small molecule inhibitor, a syngeneic knockout, and an active kinase inducible system. We applied RNA-seq and phosphoproteomic mass spectrometry to investigate the SYK-regulated EGF-induced transcriptome and downstream substrates.

Findings: Induced expression of constitutively active SYK^{130E} reduced cellular response to EGFR/ERBB2 inhibitor, lapatinib. Expression of $EGFR^{WT}$, but not SYK non-phosphorylatable $EGFR^{3F}$ mutant, resulted in paclitaxel resistance, a phenotype characteristic to SYK active ovarian cancers. In tumor xenografts, SYK inhibitor reduces phosphorylation of EGFR substrates. Compared to SYK^{WT} cells, SYK^{KO} cells have an attenuated EGFR/ERBB2-transcriptional activity and responsiveness to EGF-induced transcription. In ovarian cancer tissues, pSYK (Y525/526) levels showed a positive correlation with pEGFR (Y1187). Intense immunoreactivity of pSYK (Y525/526) correlated with poor overall survival in ovarian cancer patients.

Interpretation: These findings indicate that SYK activity positively modulates the EGFR pathway, providing a biological foundation for co-targeting SYK and EGFR.

Fund: Department of Gynecology and Obstetrics, Johns Hopkins University School of Medicine, NIH/NCI, Ovarian Cancer Research Foundation Alliance, HERA Women's Cancer Foundation and Roseman Foundation. Funders had no role in the design of the study and collection, analysis, and interpretation of data and in writing the manuscript and eventually in the decision to submit the manuscript.

1. Introduction

Ovarian high-grade serous carcinoma (HGSC) is among the most aggressive female cancers [1]. While residual tumors after tumor cytoreductive surgery are sensitive to conventional chemotherapy, most patients eventually experience recurrence, leading to high cancer-related mortality. Extensive molecular analysis has shown that nearly all HGSC tumors have somatic p53 mutations and approximately 25% have a BRCA1/2 mutation [2]. Epidermal Growth Factor Receptor (EGFR) total protein expression and amplification studies have shown significant upregulation in HGSC [3,4]. The overexpression ranges from 30 to 98% of epithelial ovarian cancer cases, while the epithelial lining of the ovary has weak EGFR expression [3]. However, EGFR did not consistently correlate with disease aggressiveness [5].

To elucidate the mechanisms underpinning how ovarian HGSCs become resistant to chemotherapy, we previously compared the

* Corresponding authors.
E-mail addresses: yu.yu@curtin.edu.au (Y. Yu), tlw@jhmi.edu (T.-L. Wang), ishih@jhmi.edu (I.-M. Shih).
[1] Current address: School of Pharmacy and Biomedical Sciences, Curtin Health Innovation Research Institute, Curtin University, Western Australia, Australia 6210.

https://doi.org/10.1016/j.ebiom.2019.08.055

Research in context

Evidence before this study

Among all gynecologic malignancies, epithelial ovarian cancer has the highest case-to-fatality ratio. Most patients are diagnosed at advanced stages and require chemotherapy after cytoreduction surgery. Recurrence is common and accounts for disease-related mortality.

Added value of this study

We identified a correlation between a higher level of nuclear active phosphorylated SYK and poor overall survival in high-grade serous ovarian carcinomas. Active SYK can phosphorylate EGFR and ERBB2 *in vitro*, and there is a positive correlation between SYK phosphorylation and EGFR phosphorylation in ovarian cancer tissues. SYK pathway activation reduced sensitivity to a dual EGFR/ERBB2 inhibitor, lapatinib, while SYK inhibition or modulated the EGF-induced transcriptome.

Implications of all the available evidence

Our data suggest that activation of SYK has an upstream role in regulating EGFR signaling and overall survival. Therefore, co-targeting SYK and EGFR appear to be an attractive target for therapeutic development in ovarian cancer.

proteomes between paired primary and recurrent post-chemotherapy HGSCs from the same women [6] to compile a list of proteins that were more frequently upregulated in recurrent tumors than in the matched primary counterparts. Among the frequently upregulated proteins, Spleen Tyrosine Kinase (SYK) was of particular interest because of its potential for therapeutic targeting with small molecular inhibitors [6]. Among SYK inhibitors, fostamatinib (prodrug of R406) has been recently approved by the U.S. Food and Drug Administration to treat idiopathic thrombocytopenia purpura, in addition to other SYK inhibitors being tested in phase 2 clinical trials for the treatment of hematopoietic malignancies [7–9]. Being the first oral SYK inhibitor, the selectivity of Fostamatinib is inferior to the newer class of SYK inhibitor, such as Entospletinib [10]. Compared to Fostamatinib, Entospletinib has increased selectivity for Janus kinase 2 (JAK-2), c-KIT, FMS-like tyrosine kinase 3 (FLT 3), RET, and VEGFR2 [11].

SYK is a non-receptor tyrosine kinase which initiates signaling *via* a number of cell surface receptors including integrins, Fc receptors, and complement receptors [12]. Several studies have suggested that SYK also participates in NFκB-mediated transcriptional regulation and in PI3K-Akt-mTOR signaling [13–17]. Biologically, SYK activity is involved in tissue inflammation *via* the SYK-PI3K pathway which has been recently reported to be the critical determinant driving proinflammatory differentiation in γδT inflammatory cytokine-producing T lymphocytes [18]. Despite the fact that SYK signaling contributes to leukemogenesis, especially in the development of acute myeloid leukemia [9], its role in solid tumors is elusive and likely dependent on the tumor types and biological contexts [19–21]. Our previous study indicated that SYK activation promotes paclitaxel resistance in ovarian cancer cells, and SYK inhibition sensitizes paclitaxel-resistant tumor cells to treatment by enhancing microtubule stability [22]. Based on these results, targeting the SYK pathway is a promising strategy for enhancing tumor responsiveness to paclitaxel. We also reported that SYK directly phosphorylates cortactin and cofilin, which are critically involved in the assembly and dynamics of actin filaments through phosphorylation signaling. In that report, we found that suppression of SYK activity inhibited ovarian tumor cell invasiveness by modulating actin dynamics [23].

In view of the diverse functions of SYK, we hypothesized that SYK activity may contribute to chemoresistance and recurrence in ovarian cancer through mechanisms in addition to the regulation of cytoskeletal dynamics. One of the important clues was based on evidence from our prior proteomic study suggesting that activated SYK phosphorylates several proteins with well-established roles in cancer pathogenesis [22]. Here, we show that both EGFR and ERBB2 are SYK phosphorylation substrates, a finding that has not been reported previously. It is well established that when phosphorylated, EGFR and ERBB2 translocate to nucleus, where they activate downstream genes that promote tumor progression in various types of epithelial cancers including ovarian carcinomas [24]. Thus, our findings reported here further our understanding of the regulation of the EGFR/ERBB2 signaling pathway. The identification of signaling cross-talk between the SYK and EGFR/ERBB2 pathways provides new insights into the pathobiology of ovarian cancer, which will impact future studies focusing on SYK-targeted therapy.

2. Materials and methods

2.1. Patient specimens

Formalin-fixed and paraffin-embedded primary HGSC tissues were obtained from the Department of Pathology at the Johns Hopkins Hospital, Baltimore, Maryland. The paraffin tissues were arranged in tissue microarrays to facilitate immunohistochemistry and to ensure that the tissues were stained under the same conditions. A total of 123 pretreated peritoneal effusions were obtained from the Norwegian Radium Hospital from patients diagnosed with serous carcinoma in the years 1998–2005. The study was approved by the Johns Hopkins University School of Medicine Institutional Review Board and the Regional Committee for Medical Research Ethics in Norway.

2.2. Correlation between SYK immuno-intensity and patient survival

For survival analyses, an H-score above the median was considered to be high expression, and an H-score below the median was considered to be low expression. To correlate the levels of nuclear pSYK and total SYK with overall patient survival, Kaplan-Meier survival analysis and log-rank test (with two-tail *p*-value) were performed; $p < .05$ was considered statistically significant. Median survival and hazard ratios with 95% CIs were also calculated.

2.3. Immunohistochemistry

The HGSC FFPE tissues were sectioned using a microtome into 4–5 μm thick on positively charged glass slides. Cells from the peritoneal fluid (ascites) were collected by centrifugation to remove the fluid. After the spin, cell blocks were created whereby the cellular pellet fixed and embedded in paraffin blocks. Sections of 4–5 μm thick were cut and stained with hematoxylin and eosin (H&E). For immunohistochemistry, the standard deparaffinization was performed, followed by antigen retrieval using a citrate-based Target Retrieval Solution (DAKO) or Trilogy™ (Cell Marque). The mouse monoclonal anti-SYK antibody [4D10.1] (Abcam #ab3113) and the polyclonal anti-phospho-SYK (Tyr525/526) antibody (Cell Signaling Technology #2711) were used. The specificity has been confirmed previously [25] and verified for this study using Western blotting as previously described [26]. Antibodies against pSTAT3 (Y705) (Cell Signaling Technology #9145), pEGFR (Y1197) (Sigma SAB4300183), pCTNNB1 (Abcam ab138378), and pERBB2(Y877) (Sigma SAB4300057) were also used. Sections were incubated with the primary antibody at 4 °C overnight, followed by the appropriate secondary antibodies at room temperature for 30 min. Colorimetric development was detected by the EnVision +System (DAKO). Immunoreactivity was scored by at least two investigators using the H-score system to minimize inter- and intra-observer variability [27]. Expression levels were determined according to the

percentage of positive tumor cells and the intensity of staining. A composite score was calculated by multiplying the extent and intensity scores.

2.4. Cell lines and viability studies

Several ovarian cancer cell lines all with detectable SYK protein expression were included in this study: SKOV3, MPSC1, EFO21, Kuramochi, OVCAR3, KK, KOC7C, OVISE, OVCA429, and OVCAR4. SKOV3 and OVCAR3 were obtained from the American Tissue Culture Center (Rockville, MD). MPSC1 cell line was previously established [28]. OVISE was obtained from the Japanese Health Science Research Resources Bank (Osaka, Japan). OVCA429, EFO21, Kuramochi, KK, KOC7C and OVCAR4 were kind gifts from Dr. B. Karlan, Cedars Sinai Medical Center, Los Angeles, California, Dr. K. Nakayama, Shimane University, Japan and Dr. S. Baylin, Johns Hopkins Medicine, Baltimore, MD. All cell lines were cultured in RPMI-1640 medium supplemented with 10% (*v*/v) fetal bovine serum and 1% penicillin/streptomycin, except for EFO21, which was maintained in the same medium with 20% (v/v) fetal bovine serum. The MPSC1TR paclitaxel resistant cell line was maintained at maximum 25 nM paclitaxel as appropriate. Prior to experiments, the paclitaxel resistant cells were washed with PBS and replenished by regular medium for a minimum of 48 h before harvesting or treating with other conditions. SKOV3 and HeLa cells expressing SYK (WT, active mutant 130E) under the Tetracycline-off (Tet-off) inducible system were generated as previously described [22]. The inducible cells were maintained under 1–2 μg/mL doxycycline to suppress SYK expression. SYK expression was induced by removing doxycycline from the cells for at least 48 h. EGFR wild-type ($EGFR^{WT}$) and mutant ($EGFR^{3F}$) were constructed into the pcDNA6/V5-His A vector. The DNA fragment containing the coding region of mutated *EGFR* gene ($EGFR^{3F}$) was synthesized by Express Mutagenesis (GenScript, NJ). The $EGFR^{WT}$ and $EGFR^{3F}$ were then transfected into $SKOV3^{130E}$ cells. For the 3D cell viability assays, 2000 cells/well were seeded in an ultra-low attachment plate (Corning) and spun at 300 ×*g* for 3 min. The cells were then incubated in RPMI-1640 medium supplemented with 10% (*v*/v) fetal bovine serum and 1% penicillin/streptomycin to promote spheroid formation. After 3 days, spheroids were treated with lapatinib (SelleckChem) at a range of concentrations for one week, after which viability was determined by the CellTiter-Glo® 3D Cell Viability Assay (Promega).

2.5. Generation of SYK knockout OVISE cells by CRISPR/Cas9 system

The pSpCas9n(BB)-2A-Puro (PX462) CRISPR/Cas9 vector from Addgene (plasmid no. 48141) was used in this study. Cloning was performed using a pair of CRISPR single-guide RNA (sgRNA) specifically targeting exon 2 of SYK: top strand-nicking sgRNA (CGGACAGGGCG AAGCCACCC) and bottom strand-nicking sgRNA (CACACCACTACACC ATCGAG), which were designed and cloned as previously described [29]. OVISE cells were transfected using Lipofectamine® 3000 (Life Technologies), and positive cells were selected in the presence of 2 μg/ml puromycin. Two to three weeks after transfection, single cell clones were isolated and screened for Cas9 expression. The knockout was verified by immunoblotting. Early passage (passage 1 or 2) knockout cells were used in experiments.

2.6. RNA isolation and reverse transcriptase-polymerase chain reaction

RNA was isolated and purified using the RNeasy Plus Mini Kit (Qiagen). The relative expression of SYK long and short isoforms in ascites tumors and cell lines was examined by reverse transcriptase followed by PCR. cDNA was synthesized using the iScript cDNA synthesis kit (BioRad), and PCR reactions were carried out using a primer set (forward, 5-AATCGGCACACAGGGAAATG-3; reverse, 5 AGCTTTCGGTC CAGGTAAAC-3) to confirm the presence of the two transcripts. PCR products corresponding to long and short SYK isoforms were semi-quantitatively analyzed after separation by 3% gel electrophoresis, followed by densitometric analyses of band intensity using Image Lab software (Bio-Rad Laboratories).

2.7. In vitro kinase assay and ADP-Glo kinase assay

For the *in vitro* kinase assay, recombinant proteins active SYK (Sigma #S6448), EGFR (Thermo #PV3872), ERBB2 (Thermo #PV3366), and CTNNB1 (Sigma #SRP5172) were added to a protein kinase buffer (50 mM Tris-HCl, 10 mM $MgCl_2$, 0.1 mM EDTA, 2 mM DTT, 0.01% Brij 35, pH 7.5) containing 100 μM ATP. The reactions were incubated at 37 °C for 1 h, and the products were separated on SDS-PAGE gels. The ADP-Glo kinase assay (Promega) was used to estimate the amount of ADP produced in the kinase reactions. Background luminescence signals arising from auto-phosphorylation or resulting from proteins alone were eliminated by subtracting signals obtained in reactions performed in the absence of SYK.

2.8. RNA isolation and RNA-seq

Isogenic OVISE ovarian cancer cell lines with SYK knockout (SYK^{KO}) were treated for 24 h with 50 ng/mL EGF (BD). RNA was isolated and purified using the RNeasy Plus Mini Kit (Qiagen). The quality of the total RNA was assessed using the Agilent 2100 Bioanalyzer RNA Nano Chip; RIN values ranged between 9.4 and 10.0. Paired-end index libraries were constructed using a standard protocol provided by Illumina. Sequencing was performed on the Illumina HiSeq2500 platform, in a 2 × 100 bp paired-end (PE) high output V4 chemistry configuration at GeneWiz, Inc. Bioinformatics analysis was performed using Galaxy, an open access web-based program that contains a variety of next-generation sequencing analysis tools. Reads were processed and aligned to *Homo sapiens* reference genome build hg19 using Tophat gapped-read mapper (ver. 2.1.0). The aligned reads were processed with Cufflinks transcript assembly (ver. 2.2.1.0), and the resulting GTF files were amalgamated to UCSC hg19 RefSeq genes annotation file using Cuffmerge (ver. 2.2.1.0). Differential expression analysis was performed using Cuffdiff (ver. 2.2.1.3) to curate a list of genes whose levels of expression changes were significantly different (q-val < 0.05) between the tested genotypes.

2.9. Animal tumor xenograft studies and phosphoproteomic mass spectrometry

SKOV3IP cells were used to establish the subcutaneous tumor xenograft model. Briefly, tumor cells were mixed with an equal volume of Matrigel (BD Biosciences) and injected subcutaneously (5×10^6 cells/injection) into 4–6 week old female nu/nu mice. Tumor growth was monitored by measuring tumor diameters and calculating tumor volume. Treatment with drugs started when tumors reached an average volume of approximately 500 mm^3. Three mice per group received intraperitoneal administration of vehicle control or R406 (10 mg/kg) four times in two days. DMSO vehicle control and R406 solution for injection were prepared in 10% 1-methyl-2-pyrrolidone, 40% PEG400, and 0.9% saline. All of the animal procedures were approved by the Johns Hopkins University Animal Care Committee. Upon completion of treatment, tumor xenografts were harvested, and snap frozen after washing with PBS containing phosSTOP.

Snap frozen tumor tissues were lysed using cold lysis buffer containing 6 M guanidine HCl, 10 mM Tris(2-carboxyethyl) phosphine HCl, 40 mM 2-chloroacetamide, and phosphatase inhibitor cocktails 2 and 3 (Sigma) in 50 mM Tris-HCl, pH 8.5. Homogenized samples were heated to 95 °C, sonicated using 3 cycles of 30 s ON/30 s OFF sonication for 3 min with the Bioruptor (Diagenode, Denville, NJ, USA), and heated again for 5 min. Insoluble material was pelleted by centrifugation, after which the protein was precipitated using a chloroform-methanol procedure and processed using a modified phase transfer surfactant aided

digestion strategy [30]. Immunoaffinity purification of phosphopeptides was carried out using anti-pTyr antibody, clone PT-66 (Sigma-Aldrich, MO). Phosphopeptide samples were subjected to a secondary digest with 1 μg of trypsin for 12 h at 37 °C. Samples were desalted using StageTips, dried *via* Speed Vac, and further enriched for phosphorylation using a PolyMAC-Ti kit according to the manufacturer's instructions (Tymora Analytical, West Lafayette, IN).

For LC-MS analysis, phosphopeptide samples were injected into an Easy nLC 1000 chromatography system coupled online to a high resolution LTQ Orbitrap Velos Pro mass spectrometer (Thermo Scientific). The phosphopeptides were separated on a 45 cm analytical column maintained at 50 °C, which was prepared using 2.1 μm ProntoSIL C18 beads (Bischoff Chromatography, Leonberg, Germany). The mass spectrometer was operated in a full MS scan (*m/z* 300–1700), followed by CID fragmentation of the top 15 most abundant ions (NCE 30%). The dynamic exclusion window was set to 10 ppm, and the exclusion time was set to 60 s. The raw LC-MS data were analyzed using the MaxQuant software version 1.5.8.3 against the Uniprot *Homo sapiens* database (downloaded August 2017). A phosphorylation site localization score of 0.75 was used as the cut-off.

2.10. Statistical analysis

Results are shown as mean ± SEM. Statistical evaluation was performed using Graphpad Prism including two-way ANOVA and Pearson correlation analysis. $p < .05$ is considered significant.

3. Results

3.1. SYK activity affects EGFR and ERBB2 phosphorylation

Based on our phospho-proteomic analysis, we found that EGFR and ERBB2 phosphorylation status was related to SYK pathway activity. Thus, we determined whether SYK affected EGFR and ERBB2 phosphorylation using *in vitro* kinase reactions and ADP-Glo kinase assay to measure ATP consumption by ADP formation. We observed a dose-dependent increase in ADP with increasing amounts of ERBB2 or EGFR added to a reaction mixture containing a fixed amount of active recombinant SYK (Fig. 1A and B), suggesting that ERBB2 and EGFR were directly phosphorylated by SYK. The estimate-specific activities were 6.4 nmole/min/mg for ERBB2 (rate constant = 46.4 min^{-1}, Mw 137,910 Da) and 48.5 nmole/min/mg for EGFR (rate constant = 361.2 min^{-1}, Mw 134,277 Da). For comparison, in control experiments, we did not observe a significant increase in SYK-dependent CTNNB1 phosphorylation (Supplemental Fig. 1A). Indeed, the ERBB2 (pY877) and EGFR (pY1197 and p Y869) phosphopeptides identified in our Stable Isotope Labeling by/with Amino acids in Cell culture (SILAC) data [22] contained acidic residues in the −1 or + 1 position adjacent to the tyrosine residues, a motif which has been implicated as a target motif for direct SYK phosphorylation [31]. We did not perform an *in vitro* kinase reaction using STAT3 because it has been previously established as a direct SYK substrate [32].

Next, we determined whether SYK was able to regulate EGFR and ERBB2 phosphorylation by measuring EGF-stimulated phosphorylation of EGFR and ERBB2 in MPSC1TR cells treated with SYK inhibitors. We found that two different SYK inhibitors, R406 (700 nM) and entospletinib (700 nM), decreased the levels of EGF-stimulated phosphorylation of EGFR (pY1197) and ERBB2 (pY877) (Fig. 1C). We also observed a corresponding reduction in the levels of p-EGFR (Y1197) and p-ERBB2 (Y877) in OVISE SYK^{KO} cells as compared to OVISE SYK^{WT} cells (Supplemental Fig. 1B). To corroborate these results, we also used the SYK Tetracycline-off (Tet-off) inducible system, in which SKOV3 was induced to express either wild-type SYK (SYK^{WT}) or a constitutively active mutant, SYK^{130E}, tagged with green fluorescent protein (GFP). The results showed that induced expression of SYK^{WT} or SYK^{130E} proteins increased the levels of pERBB2 (pY877) and pEGFR (pY1197) (Fig. 1D).

3.2. SYK interacts with EGFR/ERBB2, and its inhibition in vivo reduces phosphorylation of downstream EGFR substrates

To determine whether SYK interacts with EGFR/ERBB2 in a cellular system, we performed co-immunoprecipitation with pSYK (Y525/526) to detect the presence of pEGFR and pERBB2. The cytoplasmic, membrane, and nuclear subcellular fractions of OVISE cells, which have high endogenous levels of SYK, were immunoprecipitated using a pSYK (Y525/526) antibody (Fig. 1E). pEGFR (Y1197) and pERBB2 (Y877) levels were high in the pSYK immunoprecipitated membrane and nuclear fractions. Similar results were observed in another SYK expressing ovarian cancer cell line KOC7C (Supplemental Fig. 1C). These data suggest that pSYK interacts with these receptor kinases predominantly at the cell membrane and nucleus.

Given that active SYK phosphorylated EGFR and ERBB2 by interacting with them, we speculated that a SYK inhibitor would suppress phosphorylation of EGFR, ERBB2, and their downstream phosphorylated substrates *in vivo*. Immunocompromised nude mice bearing SKOV3IP tumor xenografts were treated with R406, and tumors were collected for global phosphoproteomic analysis. R406 treatment alone did not significantly reduce tumor growth. In total, 588 unique phosphopeptides belonging to 394 unique proteins were identified (Table S1). The numbers of unique phosphopeptides in tumor with and without R406 are 510 and 567, respectively. Fewer unique phosphopeptides were identified in tumors from the R406 treated group, presumably a consequence of inhibition of SYK kinase. The downregulated phosphoproteins included SYK itself and, importantly, EGFR and ERBB2, providing evidence that the phosphorylation of these receptor tyrosine kinases was dependent on SYK activity. In addition, phosphorylation levels of several known EGFR downstream substrates decreased in tumors from animals treated with R406; these included the adapter molecule CRK [33], 1-phosphatidylinositol 4,5-bisphosphate phosphodiesterase gamma-1 [34], hepatocyte growth factor-regulated tyrosine kinase substrate (Hrs) [35], GRB2 associated binding protein 1 (GAB1) [35], and signal transducing adapter molecule 2 (STAM2) [36] (Table S1). These findings provide compelling evidence that SYK inhibition affects EGFR phosphorylation signaling.

3.3. SYK activity promotes tumor development through EGFR signaling

Since SYK kinase activity has been shown to promote paclitaxel resistance [22], we investigated whether SYK-induced EGFR phosphorylation might also be involved. To explore this possibility, we generated a non-phosphorylatable EGFR mutant ($EGFR^{3F}$) containing phenylalanine substitutions at Y869, Y1172, and Y1197, which are the presumable SYK-dependent phosphorylation sites based on our SILAC data [22] (Table 1). In the presence of $EGFR^{WT}$, SYK^{130E}-induced cells (-Tet, expressing the constitutively active SYK^{130E}) exhibited increased resistance to paclitaxel (IC_{50} = 8.2 nM) compared to SYK^{130E} non-induced cells (+Tet; IC_{50} = 2.7 nM). In contrast, expression of the non-phosphorylatable $EGFR^{3F}$ mutant in SYK^{130E}-induced cells (-Tet) reduced paclitaxel resistance (IC_{50} = 5.4 nM) compared to cells expressing $EGFR^{WT}$ (Fig. 2A and B). These data suggest that EGFR phosphorylation is involved in SYK-induced paclitaxel resistance. Moreover, SKOV3 cells expressing SYK^{130E} were more resistant to the EGFR/ERBB2 dual kinase inhibitor, lapatinib (IC_{50s} SYK^{130E} = 150.8 μM as compared +Tet =1.8 μM), further suggesting that SYK kinase activity enhanced EGFR signaling (Fig. 2C).

3.4. SYK activity modulates the EGFR-dependent transcriptome

The signaling cross-talk between SYK and EGFR raises the possibility that SYK may indirectly regulate EGFR-mediated transcription.

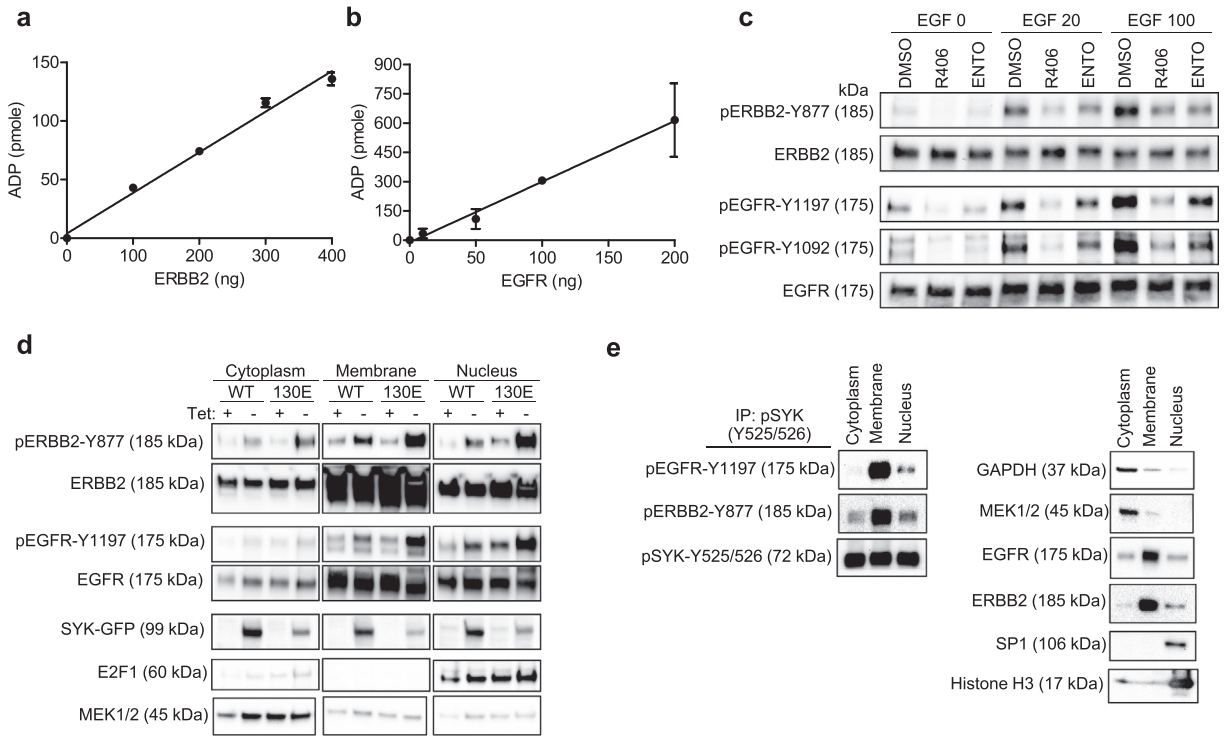

Fig. 1. SYK phosphorylates and interacts with ERBB2 and EGFR. (A and B) *In vitro* kinase assay using recombinant active SYK and ERBB2 or EGFR as indicated. ADP-Glo kinase assay was used to measure ADP produced by an *in vitro* kinase reaction using active recombinant SYK phosphorylation of ERBB2 (A), and recombinant SYK phosphorylation of EGFR protein (B). (C) MPSC1TR cells were serum starved and treated with SYK inhibitors including R406 (700 nM) and entospletinib (ENTO) (700 nM) overnight, and then induced with 0, 20, or 100 ng/mL EGF. The expression of phospho- and total ERBB2 and EGFR were determined by Western blotting. (D) SKOV3 cells ectopically expressing SYK^{WT} or SYK^{130E} active mutant under the Tet-off inducible system were fractionated, and the cytoplasmic, membrane, and nuclear fractions were analyzed for phospho- and total ERBB2 and EGFR expression using Western blotting. MEK1/2, EGFR, ERBB2, and E2F1 serve as positive controls for cytoplasmic, membrane, and nuclear fraction enrichment. (E) Co-immunoprecipitation of EGFR and ERBB2 from subcellular compartments by anti-pSYK. OVISE cells were fractionated, and cytoplasmic, membrane, and nuclear fractions were immunoprecipitated using pSYK(Y525/526) antibody. GAPDH, MEK1/2, EGFR, ERBB2, SP1 and Histone H3 serve as positive controls for cytoplasmic, membrane, and nuclear fraction enrichment.

Therefore, we generated SYK knockout OVISE ovarian cancer cells to determine if SYK kinase activity had the capacity to modulate the EGFR-dependent transcriptome. Compared to OVISE SYK^{WT} cells, OVISE SYK^{KO} cells had a reduced growth rate (Fig. 2D), as observed using two independent SYK^{KO} cells clone. We determined changes in transcript levels in well-established nuclear EGFR-regulated genes [37–41] in response to EGFR pathway activation by adding EGF to cultures of the isogenic pairs of SYK^{WT} and SYK^{KO} cells. While SYK^{WT} cells exhibited increased expression levels of *Aurora-A, cyclin D1*, *Myc*, and *COX-2* genes when stimulated by EGF, SYK^{KO} cells exhibited no significant changes after EGF treatment, indicating a failure to activate the EGFR pathway in SYK^{KO} cells (Fig. 2E). In contrast, overexpressing SYK^{130E} increased the expression levels of *Aurora-A*, *Myc* and *COX-2* genes.

To identify SYK-regulated genes and EGF responsive genes, we then performed RNA-seq using SYK^{WT} and SYK^{KO} cells with and without exogenous EGF stimulation (Fig. 3A). In the absence of EGF, we identified 1925 differentially expressed genes between SYK^{WT} and SYK^{KO} cells (termed "SYK-regulated genes") (Fig. 3B). These included 1015 upregulated and 910 downregulated genes in SYK^{KO} cells (FDR < 0.01, Table S2). Expression levels of 74 genes known to belong to the EGF/EGFR- and ERBB2-signaling pathways were altered in SYK^{KO} cells (Fig. 3C).

By comparing SYK^{WT} cells with and without EGF stimulation, we identified 1208 genes that were altered (corresponded to "EGF-responsive genes") (Fig. 3B). These included 611 upregulated and 597 downregulated genes (FDR < 0.01, Table S3) in EGF-stimulated cells. Comparison of the IPA canonical pathway between SYK-regulated and EGF-responsive genes indicated significant overlapping. We found 63.3% (19/30) of the SYK-regulated pathways were also identified as being EGF responsive pathways (Fig. 3D, Table S4 and S5).

To determine how the SYK pathway affected the response of cancer cells to EGF, we deduced a list of EGF responsive genes that become

Table 1
SYK candidate substrates with known nuclear localization and transcriptional regulator function.

Symbol	Entrez Gene Name	Phosphorylation site	SILAC ratio
RUVBL1	RuvB-like AAA ATPase 1	Y454	0.24
YBX1	Y box binding protein 1	Y72, Y158, Y162, Y208	0.25
CBL	Cbl proto-oncogene, E3 ubiquitin protein ligase	Y674	0.30
TDRD3	tudor domain containing 3	Y283	0.31
CTNNB1	catenin (cadherin-associated protein), beta 1, 88 kDa	Y489	0.32
STAT3	signal transducer and activator of transcription 3	Y705	0.32
CNBP	CCHC-type zinc finger, nucleic acid binding protein	Y101	0.34
BASP1	brain abundant, membrane attached signal protein 1	Y12	0.39
LSR	lipolysis stimulated lipoprotein receptor	Y328, Y406	0.39
EGFR	epidermal growth factor receptor	Y869, Y1110, Y1172, Y1197	≥ 0.39
ERBB2	v-erb-b2 erythroblastic leukemia viral oncogene homolog 2	Y1005, Y877	0.47

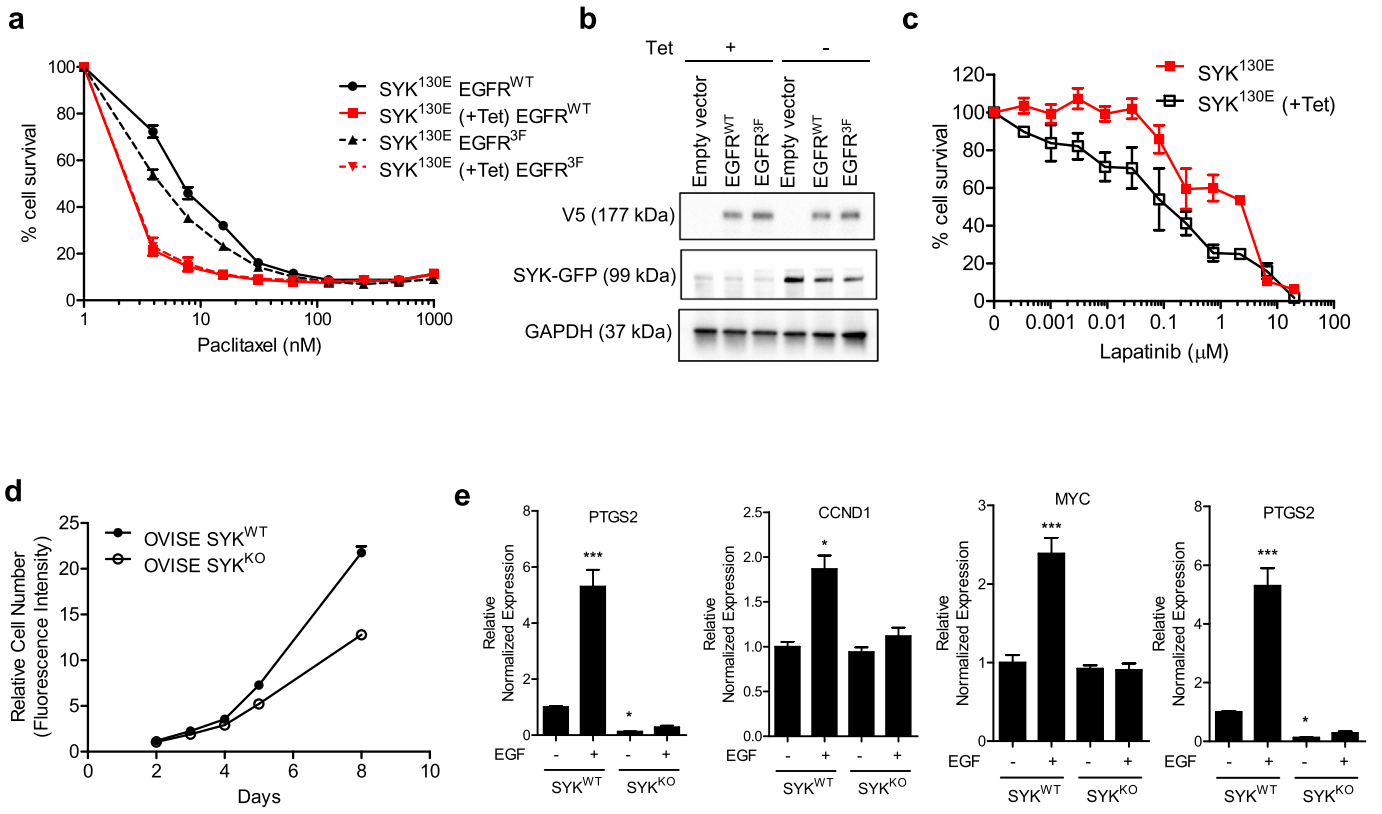

Fig. 2. EGFR signaling is responsible for SYK-mediated paclitaxel resistance. SYK activity affects lapatinib sensitivity. (A) $EGFR^{WT}$ and mutant $EGFR^{3F}$ (containing phenylalanine substitutions at Y869, Y1172, Y1197) were expressed in SKOV3 SYK^{130E} inducible Tet-off cells. Paclitaxel sensitivity was tested in 3-D spheroid culture. (B) Immunoblotting showing the expression of SYK^{130E} (GFP tag) and $EGFR^{WT}$ or $EGFR^{3F}$ (V5 tag) by cells tested in A. (C) SKOV3 SYK^{130E} Tet-off cells (±Tet) were treated with a range of lapatinib concentrations in 3-D spheroid cultures, and cell viability was examined one week later. (D) Growth curves of OVISE SYK^{WT} and syngeneic SYK^{KO} cells using the Sybr green cell proliferation assay. (E) mRNA expression of EGFR-regulated genes in OVISE SYK^{WT} and SYK^{KO} cells after stimulation with EGF (50 ng/mL) for 24 h. Cells were serum starved prior to EGF addition.

dysregulated under SYK^{KO} conditions by subtracting the EGF-responsive genes in SYK^{KO} (Table S6) from the EGF-responsive genes in SYK^{WT} cells. Among the 1208 EGF-responsive genes found to be altered in SYK^{WT} cells, 496 were also altered in SYK^{KO} cells, leaving 712 genes (58.9%) as being dysregulated by SYK knockout (Fig. 3B). Through IPA-based analysis of these 712 "SYK-dependent" genes, we identified their deduced molecular and cellular functions. Functions related to cellular movement, cell death and survival, cellular assembly and organization, cellular function and maintenance, and cell development comprised the top five (Fig. 3E). The associated canonical pathways of these "SYK-dependent" genes (Table S7) included STAT3 and PTEN pathways. These data provide further evidence of the involvement of SYK in EGFR signaling.

3.5. Correlation of phospho-SYK (Y525/526), phospho-EGFR (Y1197), and phospho-STAT3 (Y705) in human ovarian carcinoma tissues

To further determine the biological significance of SYK phosphorylation of EGFR and its downstream target, STAT3, we performed immunohistochemistry on ovarian HGSC tissues, and determined the expression patterns of pSTAT3, pEGFR, pERBB2, and pCTNNB1, using their phosphorylation site-specific antibodies. The specificity of the antibodies used was either previously reported or confirmed here by immunoblotting (Supplemental Fig. 2B—C and 3). We observed a positive correlation between nuclear pSYK (Y525/526) and nuclear p-STAT3 (Y705) ($p < .0001$ and $r = 0.45$) (Fig. 4A and B), and a positive correlation between nuclear expression of pSYK (Y525/526) and pEGFR (Y1197) ($p < .0001$; $r = 0.42$) (Fig. 4C and D). A weaker positive correlation was observed between pSYK (Y525/526) and p-ERBB2 (Y877) ($p = .049$; Pearson $r = 0.206$) (Fig. 4C and E).

We observed intense nuclear pSYK (Y525/526) immunoreactivity, and both intense cytoplasmic and nuclear total SYK immunoreactivity (Fig. 5A). To further corroborate the subcellular localization of pSYK (Y525/526) and total SYK, we isolated subcellular fractionations and found that pSYK (Y525/526) expression was abundant in the soluble nuclear fraction of all cell lines tested (OVISE, KOC7C, Kuramochi, and EFO21), but remained relatively low in the chromatin bound fraction (Fig. 5B). In addition, pSYK (Y525/526) expression was detected in the cytoskeletal fraction in the majority of the cell lines, confirming its role in cytoskeletal organization as previously reported [22]. Among all four cell lines, cytoplasmic expression of total SYK was significantly greater than nuclear expression (Fig. 5B).

3.6. SYK isoform in ovarian high grade serous carcinomas

There are two SYK isoforms, long SYK(L) and short SYK(S), distinguished by their subcellular localizations. While previous biochemical analyses showed that SYK(L) and SYK(S) had comparable intrinsic protein tyrosine kinase activity in hematopoietic cells [42], it was unclear whether the linker region (between SH2 and kinase region) present in SYK(L) but not in SYK(S) affected binding for other proteins and SYK function. For example, as compared to SYK(L), SYK(S) had reduced bind ability to phosphorylated immunoreceptor tyrosine-based activation motifs (ITAMs) [43]. In the current study, RT-PCR results showed that all 10 ovarian cancer cell lines (SKOV3, MPSC1, EFO21, Kuramochi, OVCAR3, KK, KOC7C, OVISE, OVCA429, and OVCAR4) exhibited higher expression levels of nuclear translocatable *SYK(L)* than cytoplasmic *SYK(S)* (Supplemental Fig. 5B). We extended this study to 82 ovarian cancer samples acquired from tumor ascites (Supplemental Fig. 5C and D), and observed that ovarian carcinoma cells also predominantly

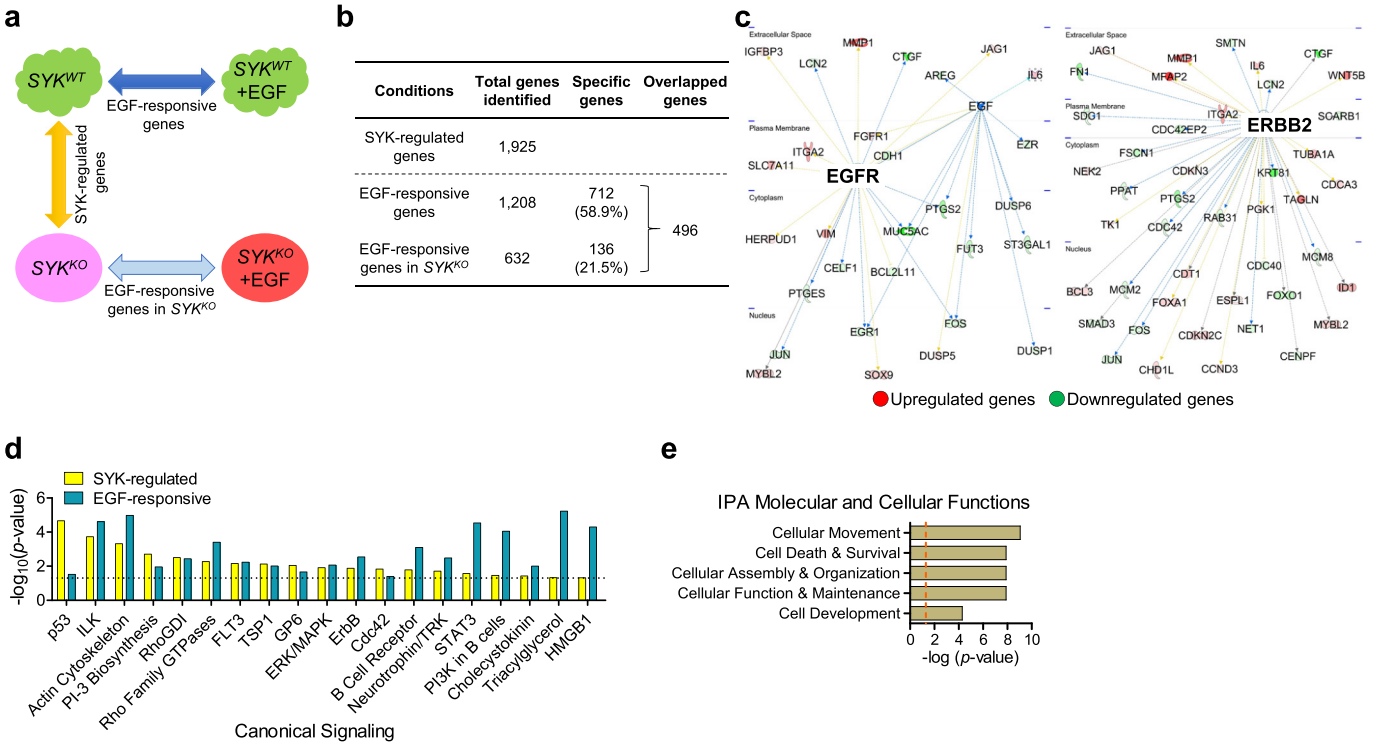

Fig. 3. Alteration of the EGF-regulated transcriptome by SYK knockout. (A) The design and comparative analyses examining differentially expressed genes between OVISE SYK^{WT} and syngeneic *SYK^{KO}* cells in the presence or absence of EGF using RNA-seq. EGF-responsive genes are obtained from comparing *SYK^{WT}* cells with and without addition of EGF (50 ng/mL). This comparison is extended to *SYK^{KO}* cells to derive EGF-responsive genes in *SYK^{KO}* condition, while comparison between *SYK^{WT}* and *SYK^{KO}* (in the absence of EGF) results in genes that are regulated by SYK. (B) Numbers of differentially expressed genes (FDR <0.01) identified as "SYK-regulated genes", "EGF-responsive genes" or "EGF-responsive genes in SYK^{KO}". (C) Ingenuity Pathway Analysis showing transcriptional network of EGFR-regulated and ERBB2-regulated genes identified among the genes that were differentially expressed between *SYK^{WT}* and *SYK^{KO}* cells. Upregulated genes are shown in red, and downregulated genes in green. (D) Top canonical signaling pathways that are shared between SYK-regulated and EGF-responsive genes. (E) Function-based analysis of the 712 "SYK-dependent" genes.

expressed SYK(L) (Supplemental Fig. 5C). *SYK(S)/SYK(L)* ratios were mostly less than one, with the exception of a single sample (Supplemental Fig. 5D). We detected *SYK(L)* expression in all samples tested, while SYK(S) was detected in only 51 (62%) of the 82 samples. These findings indicated that *SYK(L)* was the predominant isoform in ovarian cancer specimens, a result supporting the nuclear localization of pSYK in HGSC tissues.

3.7. Association between levels of pSYK (Y525/526) and clinical outcome in ovarian cancer patients

We next assessed the clinical significance of nuclear pSYK levels in two independent patient cohorts, one consisting of 42 primary HGSC tissues (with residual tumor <1 cm) from the Johns Hopkins Hospital, and the second consisting of 112 HGSC ascites samples collected from the Norwegian Radium Hospital. In both cohorts, tumors were divided into two groups according to median staining levels: low (including zero and H-scores below median) and high (H-score above median). We found that within the same cohort, tumors with higher levels of nuclear pSYK (Y525/526) were associated with shorter overall survival than those with lower levels of nuclear pSYK (Y525/526) ($p = .0074$, log-rank test) (Fig. 5C). Similarly, a positive association between high nuclear pSYK (Y525/526) and lower survival rates was found in the tumor ascites cohort ($p = .036$) Fig. 5D). The median survival in patients with low *versus* high levels of nuclear pSYK was 129 *versus* 62 months in the HGSC tissue cohort, and 28 *versus* 21 months in the HGSC ascites cohort. In addition, high nuclear pEGFR (Y1197) also correlated with lower survival rates (Fig. 5E). In contrast, total nuclear SYK levels did not impact patient survival ($p > .05$) (Fig. 5F).

4. Discussion

EGFR signaling is one of the most studied tyrosine kinase pathways in human cancer [3,44,45], and targeting its members has become a mainstay in precision cancer medicine [46,47]. Both EGFR and ERBB2 belong to the EGF receptor tyrosine kinase family. The EGFR pathway is activated upon binding of EGF to its cognate receptor localized on the cell membrane, initiating nuclear translocation and subsequent transcription regulation [48]. Their activities can be also regulated by multiple mechanisms including transcriptional upregulation by MED12 and phosphorylation by upstream kinase effectors or by collateral kinases [49]. The complexity of EGFR pathway regulation is critical for cancer cells to adapt to an ever-changing tumor microenvironment, and can explain unresponsiveness or resistance to the anti-EGFR monotherapy. As an example, EGFR and ERBB2 have been shown to be overexpressed in epithelial ovarian cancers through transcriptional upregulation and gene amplification [3,44], but clinical trials evaluating anti-EGFR or anti-ERBB2 therapies in ovarian cancer have shown minimal clinical benefit [50]. From these perspectives, the results reported here are significant, as we demonstrate that both EGFR and ERBB2 are substrates of SYK, and have shown that SYK-mediated phosphorylation enhances EGFR/ERBB2 signaling activity. These findings identify cross-talk between SYK and EGFR/ERBB2 pathways as a new translational research focus in ovarian cancer.

EGFR tyrosines can be phosphorylated by JAK2 and by ERBB2 at Y1069 [45,51] and by c-Src at Y869, Y915, Y944, Y1092, and Y1125 [52,53]. In this study, we reported novel SYK phosphorylation target sites (EGFR sites Y869, Y1110, Y1172, Y1197 and ERBB2 sites Y877, Y1005) and accordingly add additional data to map for the signaling interactome of EGFR in cancer cells. It is of interest to note that in addition

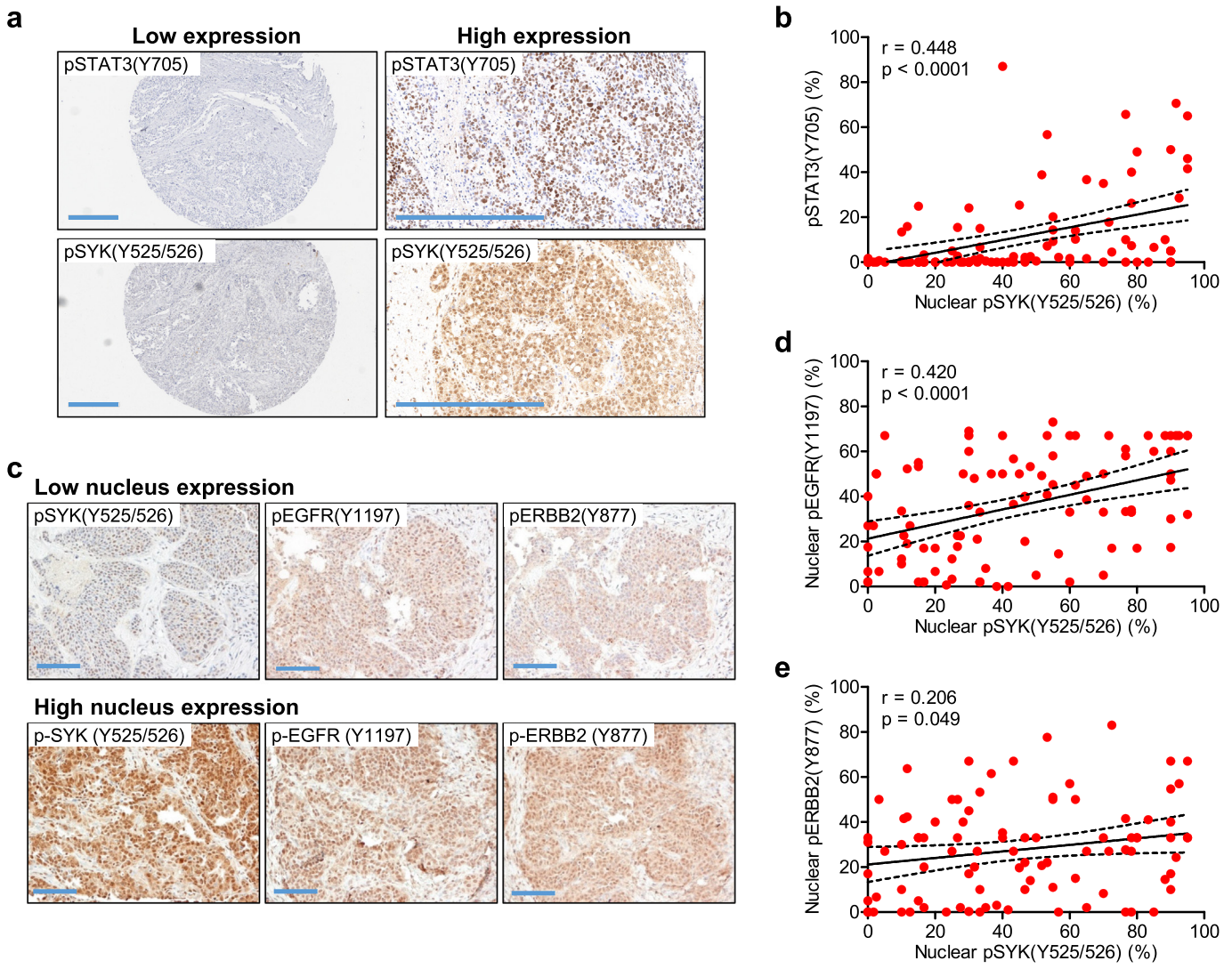

Fig. 4. Correlation of pSYK(Y525/526) with pSTAT3(Y705) and of pSYK(Y525/526) with pEGFR(Y1197) in high-grade serous ovarian carcinomas. (A) Immunohistochemical analysis of tissue microarrays containing high-grade serous carcinoma sections to detect expression of pSTAT3(Y705). The same tissues were also stained using pSYK(Y525/526) antibody ($n = 95$). Two representative tissues, one with low and one with high expression of pSYK(Y525/526) and of pSTAT3(Y705) are shown (scale bar 400 μm). (B) Association between nuclear expression levels of pSYK(Y525/526) and pSTAT3(Y705) using Pearson correlation analyses in tumors. (C) Representative photomicrographs of a high-grade serous ovarian carcinoma stained with antibodies against pSYK(Y525/526), pEGFR(Y1197), or pERBB2(Y877) (scale bar 100 μm). (D) Pearson correlation between pSYK(Y525/526) and pEGFR (Y1197). (E) Pearson correlation between pSYK(Y525/526) and pERBB2.

to EGFR/ERBB2 and STAT3, SYK also acts as an upstream kinase that phosphorylates several downstream members. This includes PIK3R1, a component of the PI3K signaling pathway, which is involved in ovarian cancer invasion and metastasis [54,55]. Thus, SYK is a molecule of potential promise for targeted therapy.

The levels of active SYK in nuclei are associated with disease aggressiveness, and inactivation of SYK using small compound inhibitors can simultaneously suppress multiple signaling pathways known to be associated with advanced malignant behaviors in human cancers (Supplemental Fig. 4). The orally efficacious SYK inhibitor, fostamatinib (prodrug of R406), has been available to treat immune-mediated thrombocytopenia purpura, and another SYK inhibitor, entospletinib (GS-9973), has been tested in clinical studies for use in treating rheumatoid arthritis and hematological malignancies [10,56–59]. Both drugs are relatively safe, with mild but reversible side effects in patients. Thus, clinical studies to test these currently available drugs to treat ovarian cancer patients warrants further consideration.

In ovarian cancer cells treated with paclitaxel, our unpublished data showed that SYK mRNA is upregulated during the breakpoint after each cycle of the chemotherapy. While the expression of pSYK can be affected by other external cues mediated by phosphorylation signaling, our current data suggest that SYK overexpression during tumor recurrence is transcriptomically regulated. While SYK is conventionally considered to be a cytoplasmic non-receptor tyrosine kinase, our data also underscore the important role of nuclear SYK, whose expression levels are associated with the aggressiveness of HGSC. The long isoform of SYK transcript contains a nuclear localization signal [60], and is the predominant form associated with ovarian cancer (Supplemental Fig. 5A-D). Similar nuclear SYK immunoreactivity can be detected in gastric carcinoma [61], hepatocellular carcinoma [62], triple negative breast carcinoma [28], and in tissues and cells of lymphoid and epithelial origins [28,62–64]. These findings raise the question of why SYK is present in the nucleus. One possibility is that SYK functions in the phosphorylation of transcriptional regulators, and is thus a regulator of their transcriptional activities [65]. Supporting this view, SYK has been reported to regulate the activity of the transcriptional regulator Ikaros and its import into the nucleus [66]. Our data showed that SYK knockout resulted in changes of EGFR-regulated genes. Thus, SYK activity can also control the transcription of downstream targets of EGFR, and can impact EGF growth factor-mediated transcription in cells.

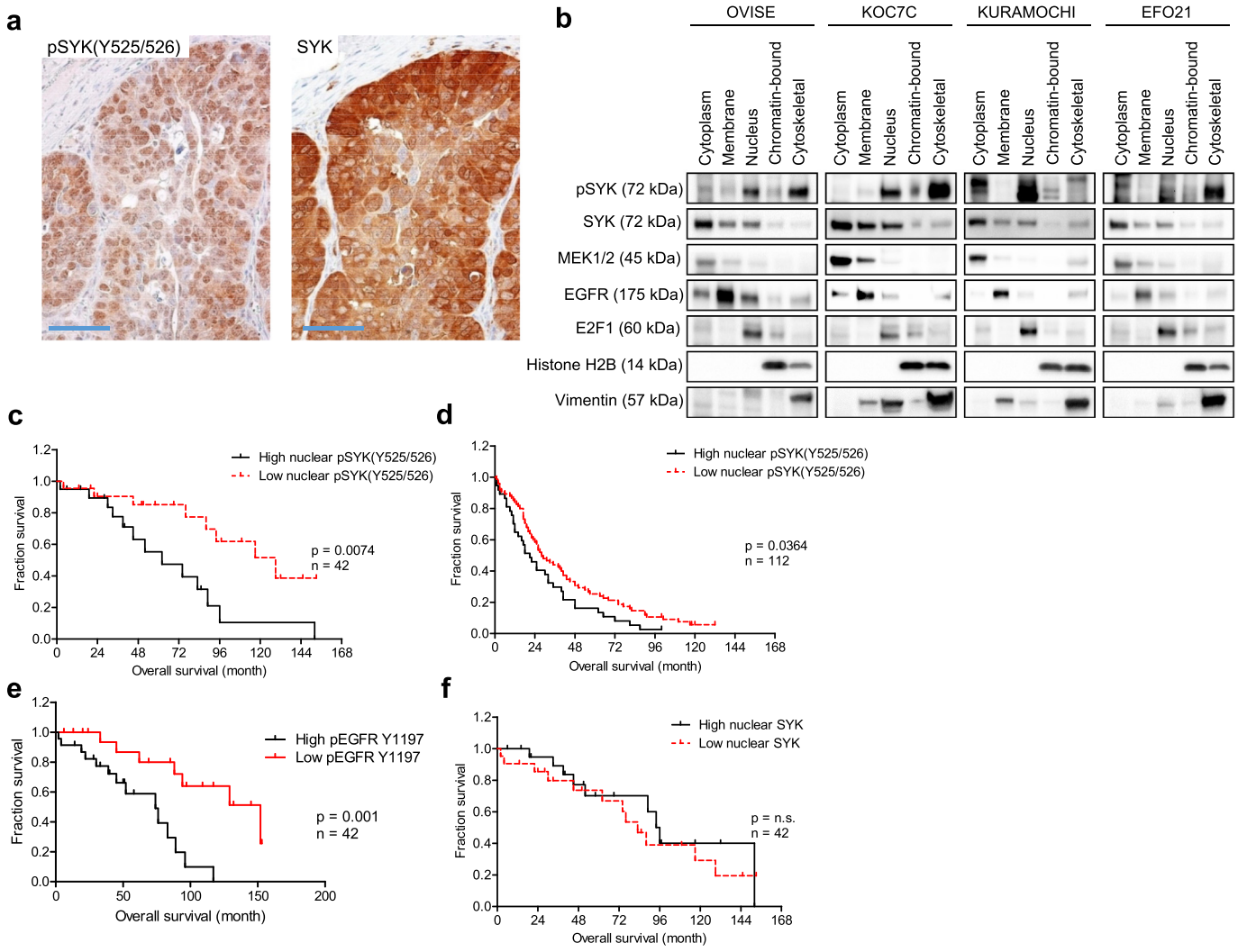

Fig. 5. Nuclear expression of active phosphorylated SYK in high grade serous ovarian carcinoma tissue and its correlation with poor survival. (A) Immunohistochemical staining of phosphorylated SYK(Y525/526) and SYK on paraffin-embedded sections of a representative high-grade serous ovarian carcinoma (scale bar 50 μm). (B) pSYK(Y525/526) if localized to nuclear and cytoskeletal cellular fractions. Ovarian cancer cell lines were subjected to subcellular fractionation and prepared for Western blot analyses. pSYK and total SYK expression in the indicated fractions were examined. MEK1, EGFR, E2F1, histone H2B, and vimentin serve as positive controls for cytoplasmic, membrane, soluble nuclear, chromatin-bound, and cytoskeletal fraction enrichment, respectively. (C – F) The association between nuclear expression of pSYK, pEGFR and SYK and overall survival in primary high-grade serous ovarian carcinoma tumors were examined by Kaplan-Meier survival analysis and log-rank test ($n = 42$). (C) Correlation of high nuclear pSYK with patient overall survival. (D) Survival analysis of patients with high *versus* low nuclear pSYK levels in pre-chemotherapy serous ovarian carcinoma peritoneal effusion samples ($n = 112$). (E) Survival analysis of patients with high *versus* low pEGFR Y1197 levels in pre-chemotherapy serous ovarian carcinoma peritoneal effusion samples (n = 42). (F) Survival analysis of patients with high *versus* low total nuclear SYK levels in primary high-grade serous ovarian carcinoma (n = 42).

The function of nuclear EGFR is more defined. It has been reported to act as a co-transcriptional activator for cyclin D1 [37], control proliferating cell nuclear antigen (PCNA) activity [67], and regulate DNA repair through DNA-PK activity [68]. In addition, several biological roles of the EGFR pathway in ovarian cancer have emerged. EGFR has been suggested to participate in promoting omental dissemination of ovarian cancer cells by inducing a paracrine loop between tumor and stromal compartments of the omental microenvironment [69]. It has been shown that inhibiting EGFR pathway activity in ovarian cancer cells is important to induce tumor dormancy [49] and targeted reduction of EGFR induces mitophagy and death of ovarian cancer cells through activation of MTOC2 and Akt [70]. The evidence shown in these studies provides a novel approach for pharmacological inhibition of EGFR activity as a potential treatment for EGFR-positive cancers. However, monotherapy targeting only the EGFR pathway may not provide an effective clinical benefit; rather, combination therapy that also includes targeting of the EGFR pathway could be promising [71]. Since SYK and EGFR may both be co-activated in HGSC tissues, and co-activation is associated with worse clinical outcomes, co-targeting these kinases may result in higher efficacy. In fact, dual inhibition of kinases has been proposed as an effective way to treat ovarian cancer in preclinical models [72]. From this perspective, the combination of EGFR inhibitor and SYK inhibitor may warrant further clinical investigation.

In summary, results presented in this report provide evidence that SYK phosphorylates the key members in the epidermal growth factor receptor (EGFR) signaling pathway, suggesting that SYK promotes tumor progression in ovarian cancer through multiple mechanisms in addition to modulating cytoskeletal proteins and their dynamics [22]. Our findings indicate that nuclear SYK activity contributes to disease aggressiveness in ovarian cancer by regulating the EGFR/ERBB2 signaling pathway. Efforts to unravel the intricate signaling interactions among SYK, EGFR/ERBB2, STAT3, and PI3K are needed to elucidate how SYK signaling orchestrates these pathways. It will be equally important to identify the nuclear proteins that are direct substrates of the SYK long isoform. Determining the effects of inhibiting SYK signaling in animal models and in future clinical trials will be crucial to determining the promise of targeting the SYK pathway using clinically available SYK inhibitors for effective cancer treatment.

Acknowledgements

This study was supported by the Richard W. TeLinde Gynecologic Laboratory (www.gynecologycancer.org) from the Department of Gynecology and Obstetrics, Johns Hopkins University School of Medicine, NIH/NCI grants, RO1CA215483 (I-M.S.) P50CA228991 (I-M.S.) and UO1CA200469 (I-M.S.), Ovarian Cancer Research Foundation Alliance (OCRFA) Grants # 458972 (I-M.S.) and #292512 (Y.Y.), and HERA OSB Grant from the HERA Women's Cancer Foundation (Y.Y.), and Roseman Foundation (I-M.S.).

Authors' contributions

Conception and design: Y. Yu, T-L. Wang, I-M. Shih; Development of methodology: Y. Yu, Y. Suryo Rahmanto; Acquisition of data: Y. Yu, Y. Suryo Rahmanto, Y-A. Shen, B. Davidson, A.N. Fader; Analysis and interpretation of data: Y. Yu, Y. Suryo Rahmanto, L. Ardighieri, A. Ayhan, B. Davidson, I-M. Shih; Writing, review, and/or revision of the manuscript: Y. Yu, S. Gaillard, T-L. Wang, I-M. Shih.

Declaration of Competing Interest

The authors report no potential conflicts of interest to disclose.

Appendix A. Supplementary data

Supplementary data to this article can be found online at https://doi.org/10.1016/j.ebiom.2019.08.055.

References

[1] Kurman RJ, Shih Ie M. The dualistic model of ovarian carcinogenesis: Revisited, Revised, and Expanded. Am J Pathol 2016;186:733–47.
[2] Integrated genomic analyses of ovarian carcinoma, Nature 2011;474:609–15.
[3] Reyes HD, Thiel KW, Carlson MJ, Meng X, Yang S, Stephan JM, et al. Comprehensive profiling of EGFR/HER receptors for personalized treatment of gynecologic cancers. Mol Diagn Ther 2014;18:137–51.
[4] Lassus H, Sihto H, Leminen A, Joensuu H, Isola J, Nupponen NN, et al. Gene amplification, mutation, and protein expression of EGFR and mutations of ERBB2 in serous ovarian carcinoma. J Mol Med (Berl) 2006;84:671–81.
[5] Mehner C, Oberg AL, Goergen KM, Kalli KR, Maurer MJ, Nassar A, et al. EGFR as a prognostic biomarker and therapeutic target in ovarian cancer: evaluation of patient cohort and literature review. Genes Cancer 2017;8:589–99.
[6] Jinawath N, Vasoontara C, Jinawath A, Fang X, Zhao K, Yap KL, et al. Oncoproteomic analysis reveals co-upregulation of RELA and STAT5 in carboplatin resistant ovarian carcinoma. PloS one 2010;5:e11198.
[7] Andorsky DJ, Kolibaba KS, Assouline S, Forero-Torres A, Jones V, Klein LM, et al. An open-label phase 2 trial of entospletinib in indolent non-Hodgkin lymphoma and mantle cell lymphoma. Br J Haematol 2018;184:215–22.
[8] Abou Dalle I, Cortes JE, Pinnamaneni P, Lamothe B, Diaz Duque A, Randhawa J, et al. A pilot phase II study of Erlotinib for the treatment of patients with relapsed/refractory acute myeloid Leukemia. Acta Haematol 2018;140:30–9.
[9] Bartaula-Brevik S, Lindstad Brattas MK, Tvedt THA, Reikvam H, Bruserud O. Splenic tyrosine kinase (SYK) inhibitors and their possible use in acute myeloid leukemia. Expert Opin Investig Drugs 2018;27:377–87.
[10] Sharman J, Hawkins M, Kolibaba K, Boxer M, Klein L, Wu M, et al. An open-label phase 2 trial of entospletinib (GS-9973), a selective spleen tyrosine kinase inhibitor, in chronic lymphocytic leukemia. Blood 2015;125:2336–43.
[11] Currie KS, Kropf JE, Lee T, Blomgren P, Xu J, Zhao Z, et al. Discovery of GS-9973, a selective and orally efficacious inhibitor of spleen tyrosine kinase. J Med Chem 2014;57:3856–73.
[12] Mocsai A, Ruland J, Tybulewicz VL. The SYK tyrosine kinase: a crucial player in diverse biological functions. Nat Rev Immunol 2010;10:387–402.
[13] Mahabeleshwar GH, Kundu GC. Syk, a protein-tyrosine kinase, suppresses the cell motility and nuclear factor kappa B-mediated secretion of urokinase type plasminogen activator by inhibiting the phosphatidylinositol 3′-kinase activity in breast cancer cells. J Biol Chem 2003;278:6209–21.
[14] Chen L, Monti S, Juszczynski P, Ouyang J, Chapuy B, Neuberg D, et al. SYK inhibition modulates distinct PI3K/AKT- dependent survival pathways and cholesterol biosynthesis in diffuse large B cell lymphomas. Cancer Cell 2013;23:826–38.
[15] Takada Y, Mukhopadhyay A, Kundu GC, Mahabeleshwar GH, Singh S, Aggarwal BB. Hydrogen peroxide activates NF-kappa B through tyrosine phosphorylation of I kappa B alpha and serine phosphorylation of p65: evidence for the involvement of I kappa B alpha kinase and Syk protein-tyrosine kinase. J Biol Chem 2003;278:24233–41.
[16] Carnevale J, Ross L, Puissant A, Banerji V, Stone RM, DeAngelo DJ, et al. SYK regulates mTOR signaling in AML. Leukemia 2013;27:2118–28.
[17] Puissant A, Fenouille N, Alexe G, Pikman Y, Bassil CF, Mehta S, et al. SYK is a critical regulator of FLT3 in acute myeloid leukemia. Cancer Cell 2014;25:226–42.
[18] Muro R, Nitta T, Nakano K, Okamura T, Takayanagi H, Suzuki H. gammadeltaTCR recruits the Syk/PI3K axis to drive proinflammatory differentiation program. J Clin Invest 2018;128:415–26.
[19] Gao P, Qiao X, Sun H, Huang Y, Lin J, Li L, et al. Activated spleen tyrosine kinase promotes malignant progression of oral squamous cell carcinoma via mTOR/S6 signaling pathway in an ERK1/2-independent manner. Oncotarget 2017;8:83900–12.
[20] Luangdilok S, Box C, Patterson L, Court W, Harrington K, Pitkin L, et al. Syk tyrosine kinase is linked to cell motility and progression in squamous cell carcinomas of the head and neck. Cancer Res 2007;67:7907–16.
[21] Repana K, Papazisis K, Foukas P, Valeri R, Kortsaris A, Deligiorgi E, et al. Expression of Syk in invasive breast cancer: correlation to proliferation and invasiveness. Anticancer Res 2006;26:4949–54.
[22] Yu Y, Gaillard S, Phillip JM, Huang TC, Pinto SM, Tessarollo NG, et al. Inhibition of spleen tyrosine kinase potentiates paclitaxel-induced cytotoxicity in ovarian Cancer cells by stabilizing microtubules. Cancer Cell 2015;28:82–96.
[23] Yu Y, Suryo Rahmanto Y, Lee MH, Wu PH, Phillip JM, Huang CH, et al. Inhibition of ovarian tumor cell invasiveness by targeting SYK in the tyrosine kinase signaling pathway. Oncogene 2018;37:3778–89.
[24] Brand TM, Iida M, Li C, Wheeler DL. The nuclear epidermal growth factor receptor signaling network and its role in cancer. Discov Med 2011;12:419–32.
[25] Cheng S, Coffey G, Zhang XH, Shaknovich R, Song Z, Lu P, et al. SYK inhibition and response prediction in diffuse large B-cell lymphoma. Blood 2011;118:6342–52.
[26] Choi JH, Park JT, Davidson B, Morin PJ, Shih Ie M, Wang TL. Jagged-1 and Notch3 juxtacrine loop regulates ovarian tumor growth and adhesion. Cancer Res 2008;68:5716–23.
[27] Ishibashi H, Suzuki T, Suzuki S, Moriya T, Kaneko C, Takizawa T, et al. Sex steroid hormone receptors in human thymoma. J Clin Endocrinol Metab 2003;88:2309–17.
[28] Pohl G, Ho CL, Kurman RJ, Bristow R, Wang TL. Shih Ie M. inactivation of the mitogen-activated protein kinase pathway as a potential target-based therapy in ovarian serous tumors with KRAS or BRAF mutations. Cancer Res 2005;65:1994–2000.
[29] Ran FA, Hsu PD, Wright J, Agarwala V, Scott DA, Zhang F. Genome engineering using the CRISPR-Cas9 system. Nat Protoc 2013;8:2281–308.
[30] Masuda T, Tomita M, Ishihama Y. Phase transfer surfactant-aided trypsin digestion for membrane proteome analysis. J Proteome Res 2008;7:731–40.
[31] Schmitz R, Baumann G, Gram H. Catalytic specificity of phosphotyrosine kinases Blk, Lyn, c-Src and Syk as assessed by phage display. J Mol Biol 1996;260:664–77.
[32] Uckun FM, Qazi S, Ma H, Tuel-Ahlgren L, Ozer Z. STAT3 is a substrate of SYK tyrosine kinase in B-lineage leukemia/lymphoma cells exposed to oxidative stress. Proc Natl Acad Sci U S A 2010;107:2902–7.
[33] Hashimoto Y, Katayama H, Kiyokawa E, Ota S, Kurata T, Gotoh N, et al. Phosphorylation of CrkII adaptor protein at tyrosine 221 by epidermal growth factor receptor. J Biol Chem 1998;273:17186–91.
[34] Kim JW, Sim SS, Kim UH, Nishibe S, Wahl MI, Carpenter G, et al. Tyrosine residues in bovine phospholipase C-gamma phosphorylated by the epidermal growth factor receptor in vitro. J Biol Chem 1990;265:3940–3.
[35] Urbe S, Sachse M, Row PE, Preisinger C, Barr FA, Strous G, et al. The UIM domain of Hrs couples receptor sorting to vesicle formation. J Cell Sci 2003;116:4169–79.
[36] Steen H, Kuster B, Fernandez M, Pandey A, Mann M. Tyrosine phosphorylation mapping of the epidermal growth factor receptor signaling pathway. J Biol Chem 2002;277:1031–9.
[37] Lin SY, Makino K, Xia W, Matin A, Wen Y, Kwong KY, et al. Nuclear localization of EGF receptor and its potential new role as a transcription factor. Nat Cell Biol 2001;3:802–8.
[38] Lo HW, Hsu SC, Ali-Seyed M, Gunduz M, Xia W, Wei Y, et al. Nuclear interaction of EGFR and STAT3 in the activation of the iNOS/NO pathway. Cancer Cell 2005;7:575–89.
[39] Hung LY, Tseng JT, Lee YC, Xia W, Wang YN, Wu ML, et al. Nuclear epidermal growth factor receptor (EGFR) interacts with signal transducer and activator of transcription 5 (STAT5) in activating Aurora-A gene expression. Nucleic Acids Res 2008;36:4337–51.
[40] Lo HW, Cao X, Zhu H, Ali-Osman F. Cyclooxygenase-2 is a novel transcriptional target of the nuclear EGFR-STAT3 and EGFRvIII-STAT3 signaling axes. Mol Cancer Res 2010;8:232–45.
[41] Jaganathan S, Yue P, Paladino DC, Bogdanovic J, Huo Q, Turkson J. A functional nuclear epidermal growth factor receptor, SRC and Stat3 heteromeric complex in pancreatic cancer cells. PloS one 2011;6:e19605.
[42] Latour S, Chow LM, Veillette A. Differential intrinsic enzymatic activity of Syk and Zap-70 protein-tyrosine kinases. J Biol Chem 1996;271:22782–90.
[43] Latour S, Zhang J, Siraganian RP, Veillette A. A unique insert in the linker domain of Syk is necessary for its function in immunoreceptor signalling. EMBO J 1998;17:2584–95.
[44] Psyrri A, Kassar M, Yu Z, Bamias A, Weinberger PM, Markakis S, et al. Effect of epidermal growth factor receptor expression level on survival in patients with epithelial ovarian cancer. Clin Cancer Res 2005;11:8637–43.
[45] Yamauchi T, Ueki K, Tobe K, Tamemoto H, Sekine N, Wada M, et al. Tyrosine phosphorylation of the EGF receptor by the kinase Jak2 is induced by growth hormone. Nature 1997;390:91–6.
[46] Hsu JL, Hung MC. The role of HER2, EGFR, and other receptor tyrosine kinases in breast cancer. Cancer Metastasis Rev 2016;35:575–88.
[47] Dokala A, Thakur SS. Extracellular region of epidermal growth factor receptor: a potential target for anti-EGFR drug discovery. Oncogene 2016;36:2337–44.
[48] Arteaga CL, Engelman JA. ERBB receptors: from oncogene discovery to basic science to mechanism-based cancer therapeutics. Cancer Cell 2014;25:282–303.

[49] Luo XL, Deng CC, Su XD, Wang F, Chen Z, Wu XP, et al. Loss of MED12 induces tumor dormancy in human epithelial ovarian Cancer via Downregulation of EGFR. Cancer Res 2018;78:3532–43.
[50] Wilken JA, Badri T, Cross S, Raji R, Santin AD, Schwartz P, et al. EGFR/HER-targeted therapeutics in ovarian cancer. Future Med Chem 2012;4:447–69.
[51] Wang SE, Narasanna A, Perez-Torres M, Xiang B, Wu FY, Yang S, et al. HER2 kinase domain mutation results in constitutive phosphorylation and activation of HER2 and EGFR and resistance to EGFR tyrosine kinase inhibitors. Cancer Cell 2006;10:25–38.
[52] Lombardo CR, Consler TG, Kassel DB. In vitro phosphorylation of the epidermal growth factor receptor autophosphorylation domain by c-src: identification of phosphorylation sites and c-src SH2 domain binding sites. Biochemistry 1995;34:16456–66.
[53] Wu W, Graves LM, Gill GN, Parsons SJ, Samet JM. Src-dependent phosphorylation of the epidermal growth factor receptor on tyrosine 845 is required for zinc-induced Ras activation. J Biol Chem 2002;277:24252–7.
[54] Meng Q, Xia C, Fang J, Rojanasakul Y, Jiang BH. Role of PI3K and AKT specific isoforms in ovarian cancer cell migration, invasion and proliferation through the p70S6K1 pathway. Cell Signal 2006;18:2262–71.
[55] Bai H, Li H, Li W, Gui T, Yang J, Cao D, et al. The PI3K/AKT/mTOR pathway is a potential predictor of distinct invasive and migratory capacities in human ovarian cancer cell lines. Oncotarget 2015;6:25520–32.
[56] Kunwar S, Devkota AR, Ghimire DK. Fostamatinib, an oral spleen tyrosine kinase inhibitor, in the treatment of rheumatoid arthritis: a meta-analysis of randomized controlled trials. Rheumatol Int 2016;36:1077–87.
[57] Weinblatt ME, Kavanaugh A, Genovese MC, Musser TK, Grossbard EB, Magilavy DB. An oral spleen tyrosine kinase (Syk) inhibitor for rheumatoid arthritis. N Engl J Med 2010;363:1303–12.
[58] Weinblatt ME, Kavanaugh A, Burgos-Vargas R, Dikranian AH, Medrano-Ramirez G, Morales-Torres JL, et al. Treatment of rheumatoid arthritis with a Syk kinase inhibitor: a twelve-week, randomized, placebo-controlled trial. Arthritis Rheum 2008;58:3309–18.
[59] Friedberg JW, Sharman J, Sweetenham J, Johnston PB, Vose JM, Lacasce A, et al. Inhibition of Syk with fostamatinib disodium has significant clinical activity in non-Hodgkin lymphoma and chronic lymphocytic leukemia. Blood 2010;115:2578–85.
[60] Wang L, Duke L, Zhang PS, Arlinghaus RB, Symmans WF, Sahin A, et al. Alternative splicing disrupts a nuclear localization signal in spleen tyrosine kinase that is required for invasion suppression in breast cancer. Cancer Res 2003;63:4724–30.
[61] Nakashima H, Natsugoe S, Ishigami S, Okumura H, Matsumoto M, Hokita S, et al. Clinical significance of nuclear expression of spleen tyrosine kinase (Syk) in gastric cancer. Cancer Lett 2006;236:89–94.
[62] Hong J, Yuan Y, Wang J, Liao Y, Zou R, Zhu C, et al. Expression of variant isoforms of the tyrosine kinase SYK determines the prognosis of hepatocellular carcinoma. Cancer Res 2014;74:1845–56.
[63] Ma H, Yankee TM, Hu J, Asai DJ, Harrison ML, Geahlen RL. Visualization of Syk-antigen receptor interactions using green fluorescent protein: differential roles for Syk and Lyn in the regulation of receptor capping and internalization. J Immunol 2001;166:1507–16.
[64] Ulanova M, Puttagunta L, Marcet-Palacios M, Duszyk M, Steinhoff U, Duta F, et al. Syk tyrosine kinase participates in beta1-integrin signaling and inflammatory responses in airway epithelial cells. Am J Physiol Lung Cell Mol Physiol 2005;288:L497–507.
[65] Mylona A, Theillet FX, Foster C, Cheng TM, Miralles F, Bates PA, et al. Opposing effects of Elk-1 multisite phosphorylation shape its response to ERK activation. Science 2016;354:233–7.
[66] Uckun FM, Ma H, Zhang J, Ozer Z, Dovat S, Mao C, et al. Serine phosphorylation by SYK is critical for nuclear localization and transcription factor function of Ikaros. Proc Natl Acad Sci U S A 2012;109:18072–7.
[67] Wang SC, Nakajima Y, Yu YL, Xia W, Chen CT, Yang CC, et al. Tyrosine phosphorylation controls PCNA function through protein stability. Nat Cell Biol 2006;8:1359–68.
[68] Chen DJ, Nirodi CS. The epidermal growth factor receptor: a role in repair of radiation-induced DNA damage. Clin Cancer Res 2007;13:6555–60.
[69] Lau TS, Chan LK, Wong EC, Hui CW, Sneddon K, Cheung TH, et al. A loop of cancer-stroma-cancer interaction promotes peritoneal metastasis of ovarian cancer via TNFalpha-TGFalpha-EGFR. Oncogene 2017;36:3576–87.
[70] Katreddy RR, Bollu LR, Su F, Xian N, Srivastava S, Thomas R, et al. Targeted reduction of the EGFR protein, but not inhibition of its kinase activity, induces mitophagy and death of cancer cells through activation of mTORC2 and Akt. Oncogenesis 2018;7:5.
[71] Lheureux S, Krieger S, Weber B, Pautier P, Fabbro M, Selle F, et al. Expected benefits of topotecan combined with lapatinib in recurrent ovarian cancer according to biological profile: a phase 2 trial. Int J Gynecol Cancer 2012;22:1483–8.
[72] Simpkins F, Jang K, Yoon H, Hew KE, Kim M, Azzam DJ, et al. Dual Src and MEK inhibition decreases ovarian Cancer growth and targets tumor initiating stem-like cells. Clin Cancer Res 2018;24:4874–86.